Lecture 35: Random braids and winding numbers

1 Random walks on Cayley graphs

A physical braid is a collection of strands that are anchored at both ends.

$$\sigma_i\sigma_j = \sigma_j\sigma_i \quad \text{for} \quad |i-j| > 1; \qquad \sigma_i\sigma_j\sigma_i = \sigma_j\sigma_i\sigma_j \quad \text{for} \quad |i-j| = 1. \tag{1}$$

A convenient representation of a group is given by its *Cayley graph*. Figure 2(a) shows part of the Cayley graph for B_3: the identity is at the center, and moving by one step north, south, east, or west in the graph corresponds to multiplication by σ_1, σ_1^{-1}, σ_2, or σ_2^{-1}, respectively. At first glance, the Cayley graph would appear to be a tree, but the braid group relations (1) imply that we sometimes get the same element along different branches, or even return to the identity (since, for example, $\sigma_1\sigma_2\sigma_1\sigma_2^{-1}\sigma_1^{-1}\sigma_2^{-1} = e$). The graph thus has a very complicated topology.

A random walk on a Cayley graph is defined by starting from some group element and repeatedly moving in a random direction, typically with equal probability, to generate a random sequence of generators. We can then ask typical questions, such

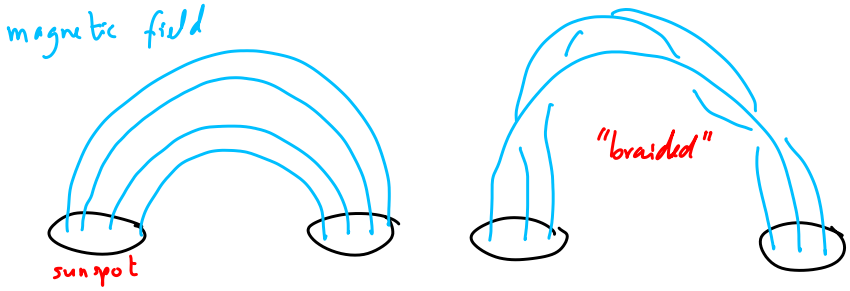

Figure 1: Magnetic flux tubes.

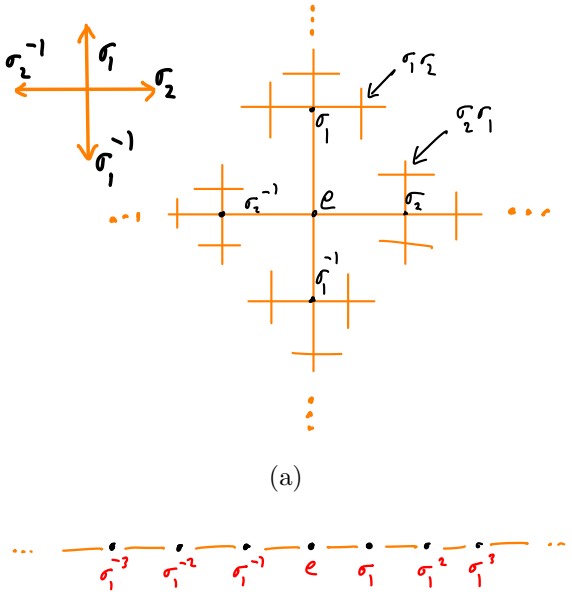

(a)

(b)

Figure 2: (a) Cayley graph for B_3. (b) Cayley graph for B_2.

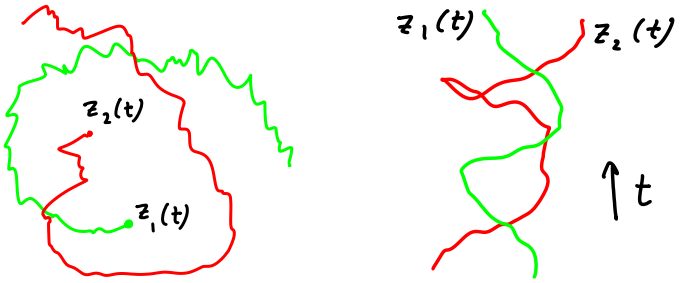

(a) (b)

Figure 3: (a) Two Brownian particles winding around each other. (b) Lifted trajectories, with 'time' running vertically.

as the probability of recurrence, or if the walk is not recurrent we can ask about the asymptotic distance from our starting point. Random walks on Cayley graphs are also used to generate braids to study polymer entanglement, and their 'complexity' is gauged by the asymptotic behavior of a knot polynomial associated with the closure of the braid (Nechaev, 1996).

By far the simplest graph, though, is that of B_2, depicted in Figure 2(b). Here we can only twist the two strands in one direction or the other, so the braid after N steps in the graph is σ_1^m, where m is a random variable with binomial distribution

$$P_N(m) = \binom{N}{(N+m)/2} p^{(N+m)/2}(1-p)^{(N-m)/2}, \qquad m+N \text{ even}, \tag{2}$$

and $P_N(m) = 0$ if $m + N$ is odd. Here p is the probability of moving right in the graph, and $(1-p)$ is the probability of moving left. The mean of m is $N(p-\frac{1}{2})$, and its variance is $Np(1-p)$. For large N, $P_N(m)$ will converge to a normal distribution.

2 Braid of two Brownian particles

Let us formulate a somewhat more 'physical' version of the random walk on B_2 discussed at the end of the previous section. Consider two Brownian particles on the plane, $z_1(t)$ and $z_2(t)$, each with diffusion constant D (Figure 3(a)). We can regard these as a braid with two strands by plotting the trajectories with time as a vertical axis, as in Figure 3(b). How is the resulting random braid distributed for large time?

For two strands all that matters is the winding angle of one particle around the other. We consider the vector $z(t) = z_1(t) - z_2(t)$, which behaves like a Brownian

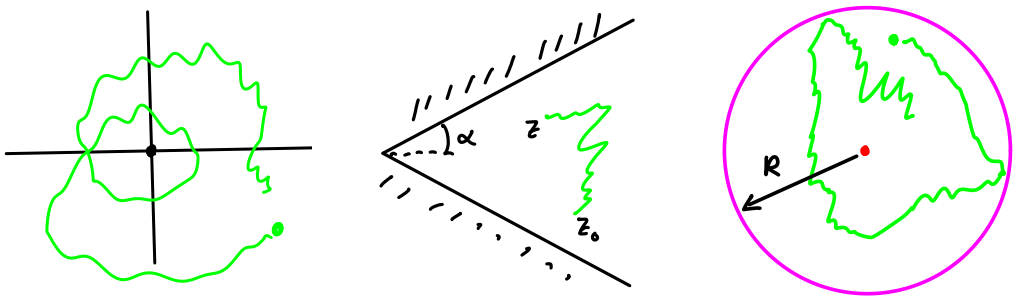

(a) (b) (c)

Figure 4: (a) A single Brownian particle winding around the origin. (b) A particle starting at z_0 and ending at z in a wedge-shaped domain. (c) Particle in a disk of radius R, with reflecting boundaries.

particle of diffusivity $2D$. We define $\theta \in (-\infty, \infty)$ to be the total winding angle of $z(t)$ around the origin. The geometrical relationship between m from Section 1 and θ is $\theta = \pi m$, though their distributions are very different. The time-asymptotic distribution of θ is given by the classical Spitzer formula (Spitzer, 1958),

$$P(x) = \frac{1}{\pi}\frac{1}{1+x^2}\,, \qquad x := \frac{2\theta}{\log(4Dt/r_0^2)}\,, \qquad 4Dt/r_0^2 \gg 1, \tag{3}$$

where $r_0 = |z(0)|^2$. This result can be derived from conformal invariance of the Brownian process (Drossel & Kardar, 1996), or by solving the heat equation in polar coordinates in the interior of a wedge-shaped domain (Fig. 4(b)), then taking the wedge angle to infinity (Edwards, 1967; Redner, 2001). Going around the origin then corresponds to moving to a different Riemann sheet. See Appendix A for a derivation.

Equation 3 is a Cauchy–Lorentz distribution, which has mean zero but an infinite variance (all even moments diverge; the odd moments are zero by symmetry if the integrals are interpreted as principal values). This peculiarity can be traced to the 'scale-free' nature of a Brownian process: since the particle motion is rough at all scales, if it comes near the origin it can wind an infinite number of times around the origin in finite time.

A straightforward numerical simulation of a Brownian particle yields the winding angle distribution in Fig. 6(b). Also shown is the Spitzer formula (3); the agreement is good for small θ, but the tails are off by a wide margin. The discrepancy is due to the numerical difficulty of recreating a true Brownian process: we cannot have an

unbounded number of windings in a small time. Thus, the observed distribution has exponential tails rather than a power-law. Bélisle (1989) derived the distribution for a small (but finite) step size:

$$P(x) = \tfrac{1}{2}\,\mathrm{sech}\,(\pi x/2)\,, \qquad 4Dt/r_0^2 \gg 1, \tag{4}$$

with x defined as in (3). Notice that the step size does not enter the formula (for large time). The same distribution applies to a Brownian process winding around a small disk centered on the origin, even as the disk radius is taken to zero. Most regularizations that prevent infinite winding around the origin will turn (3) into (4). The latter is this the proper 'physical' distribution, since physical entities such as magnetic field lines are not true Brownian processes.

A Derivation of Spitzer's law

Consider the two-dimensional diffusion equation

$$\frac{\partial v}{\partial t} - D\Delta v = \frac{1}{r_0}\,\delta(r - r_0)\,\delta(\theta - \theta_0)\,\delta(t) \tag{5}$$

for the Green's function $v(r, \theta, t)$. This equation has Laplace transform

$$s\bar{v} - D\Delta\bar{v} = \frac{1}{r_0}\,\delta(r - r_0)\,\delta(\theta - \theta_0) \tag{6}$$

where $\bar{v}(r, \theta, s)$ is the Laplace transform of $v(r, \theta, t)$. The free space Green's function is

$$v(x, y, t \,|\, x_0, y_0, 0) = \frac{1}{4\pi Dt}\,\mathrm{e}^{-R^2/4Dt} \tag{7}$$

with Laplace transform

$$\bar{v}(x, y, s \,|\, x_0, y_0) = \frac{1}{2\pi D}\,K_0(R\,q) \tag{8}$$

where K_0 is a modified Bessel function of the second kind, and

$$q = \sqrt{s/D}, \qquad R^2 = (x - x_0)^2 + (y - y_0)^2 = r^2 + r_0^2 - 2rr_0\cos(\theta - \theta_0). \tag{9}$$

We wish to find the Green's function in an infinite domain, but over multiple Riemann sheets. We write $v = u + w$ and solve for w, which satisfies the homogeneous equation

$$\frac{\partial w}{\partial t} - D\Delta w = 0, \qquad \text{or} \qquad s\bar{w} - D\Delta\bar{w} = 0, \tag{10}$$

and vanishes at $t = 0$. Assume the separable form

$$\bar{w} = \mathcal{R}(r)\mathcal{T}(\theta). \tag{11}$$

Then using

$$\Delta\bar{w} = \frac{\partial^2\bar{w}}{\partial r^2} + \frac{1}{r}\frac{\partial\bar{w}}{\partial r} + \frac{1}{r^2}\frac{\partial^2\bar{w}}{\partial\theta^2} \tag{12}$$

we find

$$\Delta\bar{w} = \mathcal{T}\mathcal{R}'' + \frac{\mathcal{T}\mathcal{R}'}{r} + \frac{\mathcal{R}\mathcal{T}''}{r^2} = q^2\mathcal{R}\mathcal{T} \tag{13}$$

or

$$\frac{r^2\mathcal{R}''}{\mathcal{R}} + \frac{r\mathcal{R}'}{\mathcal{R}} - r^2q^2 = -\frac{\mathcal{T}''}{\mathcal{T}} = \nu^2. \tag{14}$$

The angular part is

$$\mathcal{T}'' + \nu^2\mathcal{T} = 0, \tag{15}$$

with independent solutions

$$\mathcal{T} = \cos\nu\theta \quad \text{and} \quad B\sin\nu\theta, \tag{16}$$

whilst the radial part satisfies Bessel's equation

$$r^2\mathcal{R}'' + r\mathcal{R}' - \left(q^2r^2 + \nu^2\right)\mathcal{R} = 0. \tag{17}$$

The solutions are

$$\mathcal{R} = K_\nu(qr) \quad \text{and} \quad I_\nu(qr). \tag{18}$$

The solution that is regular at the origin, vanishes at ∞, and is continuous at $r = r_0$ is

$$\mathcal{R} = K_\nu(qr_>)\, I_\nu(qr_<) \tag{19}$$

where $r_> = r$ for $r > r_0$, $r_> = r_0$ for $r < r_0$ (vice versa for $r_<$). Now use this formula from Carslaw & Jaeger (1959, eq. 14.14(1)):

$$K_0(R\,q) = P\int_{-\mathrm{i}\infty}^{\mathrm{i}\infty} \frac{\cos\nu(\pi - \theta + \theta_0)}{\sin\nu\pi} K_\nu(qr)I_\nu(qr_0)\,\mathrm{i}\,\mathrm{d}\nu, \qquad r > r_0, \tag{20}$$

where P denotes the principal value at the origin, which suggests we write $\bar{w}$ as

$$\bar{w} = \frac{1}{2\pi D}\,P\int_{-\mathrm{i}\infty}^{\mathrm{i}\infty} \left(A(\nu)\cos\nu\theta + B(\nu)\sin\nu\theta\right) K_\nu(qr)I_\nu(qr_0)\,\mathrm{i}\,\mathrm{d}\nu \tag{21}$$

and choose $A(\nu)$ and $B(\nu)$ to satisfy the boundary conditions. The Green's function $\bar{v} = \bar{u} + \bar{w}$ is then

$$\bar{v} = \frac{1}{2\pi D} P \int_{-\mathrm{i}\infty}^{\mathrm{i}\infty} \left(A(\nu) \cos \nu\theta + B(\nu) \sin \nu\theta + \frac{\cos \nu(\pi - \theta + \theta_0)}{\sin \nu\pi} \right) K_\nu(qr) I_\nu(qr_0) \, \mathrm{i} \, \mathrm{d}\nu. \tag{22}$$

Let's try to satisfy the zero condition at $\theta = 0$ and $\theta = \gamma$, as in C&J. At $\theta = \gamma$,

$$\bar{v} = \frac{1}{2\pi D} P \int_{-\mathrm{i}\infty}^{\mathrm{i}\infty} \Bigg(A(\nu) \cos \nu\gamma + B(\nu) \sin \nu\gamma + \frac{\cos \nu(\pi - \gamma + \theta_0)}{\sin \nu\pi} \Bigg) K_\nu(qr) I_\nu(qr_0) \, \mathrm{i} \, \mathrm{d}\nu = 0 \tag{23}$$

so

$$B(\nu) = -\frac{A(\nu) \sin \nu\pi \cos \nu\gamma + \cos \nu(\pi - \gamma + \theta_0)}{\sin \nu\pi \sin \nu\gamma} \, . \tag{24}$$

At $\theta = 0$,

$$\bar{v} = \frac{1}{2\pi D} P \int_{-\mathrm{i}\infty}^{\mathrm{i}\infty} \left(A(\nu) + \frac{\cos \nu(\pi + \theta_0)}{\sin \nu\pi} \right) K_\nu(qr) I_\nu(qr_0) \, \mathrm{i} \, \mathrm{d}\nu = 0. \tag{25}$$

We need to be careful here: solving for $A(\nu)$ to make the expression in parentheses vanish is possible but leads to $\bar{w} = -\bar{u}$, so $\bar{v} = 0$. What we have to to is to choose $A(\nu)$ to remove the pole in the denominator when $\theta = 0$:

$$A(\nu) = -\frac{\cos \nu(\pi - \theta_0)}{\sin \pi\nu}. \tag{26}$$

After combining those two expressions, we find

$$\bar{v} = -\frac{1}{\pi D} \int_{-\mathrm{i}\infty}^{\mathrm{i}\infty} \frac{\sin \nu(\gamma - \theta) \sin \nu\theta_0}{\sin \nu\gamma} K_\nu(qr) I_\nu(qr_0) \, \mathrm{i} \, \mathrm{d}\nu. \tag{27}$$

where we removed the principal value since the integral is now regular at $\nu = 0$. This is the 2D version of 14.14(3) in C&J. We evaluate the integral by closing the contour on the right and summing the residues. We obtain the residues from

$$\frac{\sin \nu(\gamma - \theta)}{\sin \nu\gamma} \sim \frac{\sin \nu_k(\gamma - \theta)}{(-1)^k \gamma(\nu - \nu_k)} = -\frac{\sin \nu_k\theta}{\gamma(\nu - \nu_k)}, \quad \nu \text{ near } \nu_k = \pi k/\gamma, \tag{28}$$

which leads to

$$\bar{v} = \frac{2}{\gamma D} \sum_{k=1}^{\infty} \sin(\nu_k\theta) \sin(\nu_k\theta_0) \, K_{\nu_k}(qr) I_{\nu_k}(qr_0), \qquad \nu_k = \pi k/\gamma, \tag{29}$$

valid for $r > r_0$ and $0 \le \theta \le \gamma$. We can use the symmetry of the Green's function to write

$$\bar{v} = \frac{2}{\gamma D} \sum_{k=1}^{\infty} \sin(\nu_k \theta) \sin(\nu_k \theta_0) K_{\nu_k}(q r_>) I_{\nu_k}(q r_<), \qquad 0 \le \theta \le \gamma, \tag{30}$$

valid for $0 < r < \infty$. Using formula 22 from Appendix V of C&J, we can invert the Laplace transform to obtain finally

$$v = \frac{1}{\gamma D t} \, \mathrm{e}^{-(r^2+r_0^2)/4Dt} \sum_{k=1}^{\infty} \sin(\nu_k \theta) \sin(\nu_k \theta_0) \, I_{\nu_k}\Big(\frac{r r_0}{2Dt}\Big) \qquad 0 \le \theta \le \gamma. \tag{31}$$

We can center the wedge so that it extends between $-\gamma/2 \le \theta \le \gamma/2$ by replacing θ by $\theta + \gamma/2$:

$$v = \frac{1}{\gamma D t} \, \mathrm{e}^{-(r^2+r_0^2)/4Dt} \left(\sum_{k \text{ even}}^{\infty} \sin(\nu_k \theta) \sin(\nu_k \theta_0) + \sum_{k \text{ odd}}^{\infty} \cos(\nu_k \theta) \cos(\nu_k \theta_0) \right) I_{\nu_k}\Big(\frac{r r_0}{2Dt}\Big), \tag{32}$$

valid for $-\gamma/2 \le \theta, \theta_0 \le \gamma/2$. This may appear more cumbersome but now we can take the limit $\gamma \to \infty$ while keeping θ and θ_0 finite. The difference between two successive ν_k is

$$\mathrm{d}\nu_k = \nu_{k+2} - \nu_k = 2\pi/\gamma. \tag{33}$$

Thus, in the limit as $\gamma \to \infty$,

$$v = \frac{1}{2\pi D t} \, \mathrm{e}^{-(r^2+r_0^2)/4Dt} \int_0^{\infty} \left(\sin(\nu\theta) \sin(\nu\theta_0) + \cos(\nu\theta) \cos(\nu\theta_0) \right) \, I_{\nu}\Big(\frac{r r_0}{2Dt}\Big) \, \mathrm{d}\nu. \tag{34}$$

or

$$v = \frac{1}{2\pi D t} \, \mathrm{e}^{-(r^2+r_0^2)/4Dt} \int_0^{\infty} \cos \nu(\theta - \theta_0) \, I_{\nu}\Big(\frac{r r_0}{2Dt}\Big) \, \mathrm{d}\nu. \tag{35}$$

This form is equivalent to (see Duffy (2001, p. 215))

$$v = \frac{1}{\pi} \int_0^{\infty} \cos \nu(\theta - \theta_0) \int_0^{\infty} \alpha J_{\nu}(\alpha r) J_{\nu}(\alpha r_0) \, \mathrm{e}^{-D\alpha^2 t} \, \mathrm{d}\alpha \, \mathrm{d}\nu. \tag{36}$$

At $t = 0$ we can use (see `http://functions.wolfram.com/Bessel-TypeFunctions/BesselJ/21/02/02/`)

$$\int_0^{\infty} \alpha J_{\nu}(\alpha r) J_{\nu}(\alpha r_0) \, \mathrm{d}\alpha = \frac{1}{r} \, \delta(r - r_0), \qquad \frac{1}{\pi} \int_0^{\infty} \cos \nu(\theta - \theta_0) \, \mathrm{d}\nu = \delta(\theta - \theta_0) \tag{37}$$

to explicitly recover the delta-function initial condition from (36). We can also show that the normalization is preserved. Reversing the role of α and r, ν and θ in (37), we have

$$\int_0^\infty r J_0(\alpha r)\, \mathrm{d}r = \int_0^\infty r J_0(\alpha r) J_0(0r)\, \mathrm{d}r = \frac{1}{\alpha}\,\delta(\alpha), \tag{38}$$

and

$$\frac{1}{\pi}\int_{-\infty}^{\infty} \cos\nu(\theta-\theta_0)\,\mathrm{d}\theta = 2\delta(\nu)\,, \tag{39}$$

but note that $\int_0^\infty \delta(\nu)\,\mathrm{d}\nu = 1/2$, so the factor of 2 in (39) cancels out upon integration. Together these give

$$\begin{aligned}\int_0^\infty \int_{-\infty}^{\infty} rv\,\mathrm{d}\theta\,\mathrm{d}r &= \int_0^\infty \int_0^\infty \alpha r J_0(\alpha r) J_0(\alpha r_0)\,\mathrm{e}^{-D\alpha^2 t}\,\mathrm{d}\alpha\,\mathrm{d}r \\ &= \int_0^\infty \delta(\alpha) J_0(\alpha r_0)\,\mathrm{e}^{-D\alpha^2 t}\,\mathrm{d}\alpha = 1.\end{aligned}$$

Let's rewrite the PDF (35) in terms of the scaled variables $x = r/2\sqrt{Dt}$, $y = r_0/2\sqrt{Dt}$, and write θ for $\theta - \theta_0$ without loss of generality:

$$p = \frac{2}{\pi}\,\mathrm{e}^{-(x^2+y^2)} \int_0^\infty \cos\nu\theta\, I_\nu(2xy)\,\mathrm{d}\nu. \tag{40}$$

Since $2xy$ is small, we use the asymptotic form

$$I_\nu(x) \sim \frac{1}{\Gamma(\nu+1)}\,(x/2)^\nu \tag{41}$$

and the integral

$$\int_0^\infty \cos\nu\theta\,\xi^\nu\,\mathrm{d}\nu = -\frac{\log\xi}{\theta^2+\log^2\xi}, \qquad 0<\xi<1 \tag{42}$$

to obtain

$$p \simeq -\frac{2}{\pi}\,\frac{\log(xy)}{\theta^2+\log^2(xy)}\,\mathrm{e}^{-(x^2+y^2)}. \tag{43}$$

The most interesting thing to us is the total probability of reaching a certain angle θ for any x, so we integrate over x using $\log x \ll \log y$, since y is very small whereas x varies from 0 to ∞. Thus,

$$\int_0^\infty x\,p\,\mathrm{d}x \approx \frac{1}{\pi}\,\frac{-\log y}{\theta^2+\log^2 y}, \qquad y = \frac{r_0}{2\sqrt{Dt}} \ll 1, \tag{44}$$

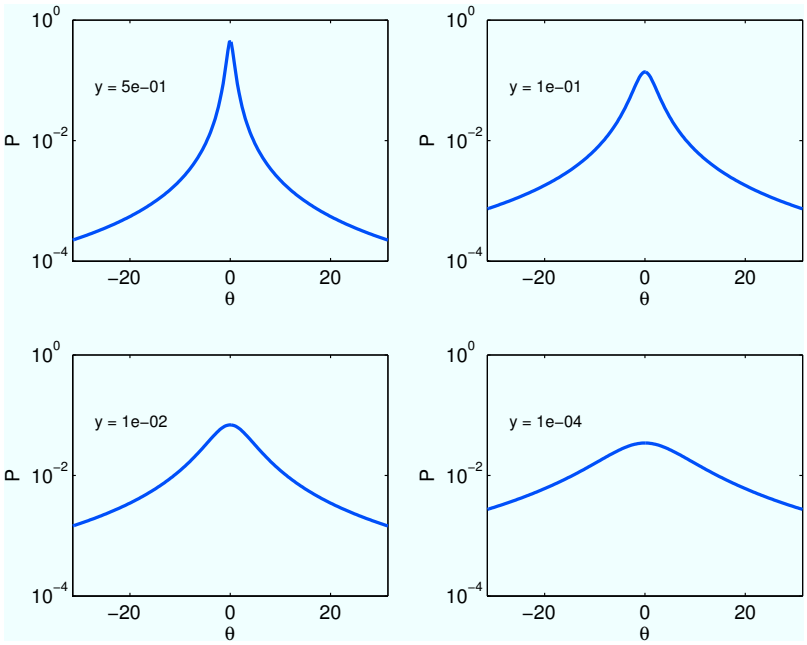

Figure 5: The Cauchy–Lorentz distribution (44) for various y values.

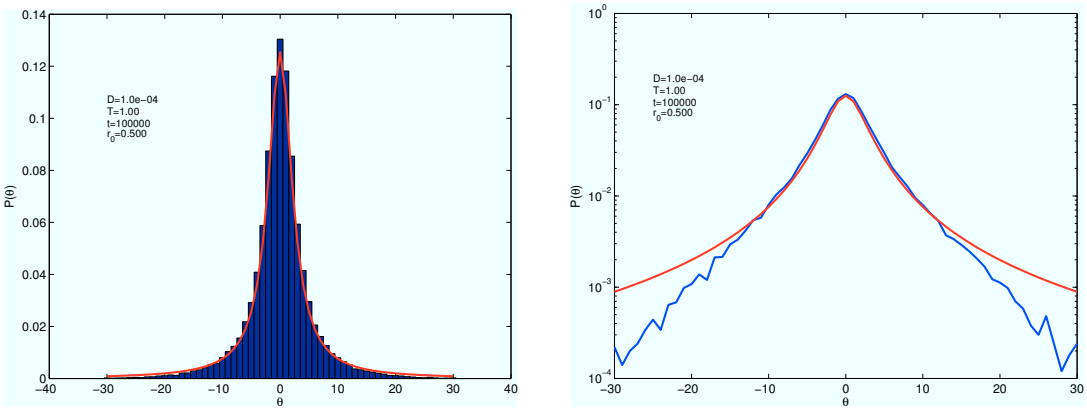

(a) (b)

Figure 6: Spitzer distribution compared to numerical simulation.

where we also approximated $\mathrm{e}^{-y^2} \simeq 1$, to obtain a consistent normalization in θ.

The PDF (44) is a Cauchy–Lorentz distribution in θ (see Fig. 5). This is the probability of finding the particle at θ at time t, given that it started at $\theta = 0$ and radius r_0. The distribution is singular at $y = 0$: if the particle starts at the origin, then it's impossible to define its Riemann sheet. The form (44) compares favorably with numerical simulations (Fig. 6(a)), though there are problems with the tails, as is obvious in Fig. 6(b).

References

Aref, H. 1984 Stirring by chaotic advection. *J. Fluid Mech.* **143**, 1–21.

Bélisle, C. 1989 Windings of random walks. *Ann. Prob.* **17** (4), 1377–1402.

Bélisle, C. & Faraway, J. 1991 Winding angle and maximum winding angle of the two-dimensional random walk. *J. Appl. Prob.* **28** (4), 717–726.

Berger, M. A. 1987 The random walk winding number problem: convergence to a diffusion process with excluded area. *J. Phys. A* **20**, 5949–5960.

Berger, M. A. & Roberts, P. H. 1988 On the winding number problem with finite steps. *Adv. Appl. Prob.* **20** (2), 261–274.

Carslaw, H. S. & Jaeger, J. G. 1959 *Conduction of heat in solids*, 2nd edn. Oxford, U.K.: Oxford University Press.

Drossel, B. & Kardar, M. 1996 Winding angle distributions for random walks and flux lines. *Phys. Rev. E* **53** (6), 5861–5871.

Duffy, D. G. 2001 *Green's functions with applications*. Boca Raton, FL: Chapman & Hall/CRC Press.

Edwards, S. F. 1967 Statistical mechanics with topological constraints: I. *Proc. Phys. Soc.* **91**, 513–519.

Fisher, M. E., Privman, V. & Redner, S. 1984 The winding angle of planar self-avoiding walks. *J. Phys. A* **17**, L569.

Grosberg, A. & Frisch, H. 2003 Winding angle distribution for planar random walk, polymer ring entangled with an obstacle, and all that: Spitzer-Edwards-Prager-Frisch model revisited. *J. Phys. A* **36** (34), 8955–8981.

Nechaev, S. K. 1996 *Statistics of Knots and Entangled Random Walks*. Singapore; London: World Scientific.

Pitman, J. & Yor, M. 1986 Asymptotic laws of planar Brownian motion. *Ann. Prob.* **14** (3), 733–779.

Pitman, J. & Yor, M. 1989 Further asymptotic laws of planar Brownian motion. *Ann. Prob.* **17** (3), 965–1011.

Pontin, D. I., Wilmot-Smith, A. L., Hornig, G. & Galsgaard, K. 2011 Dynamics of braided coronal loops. II. Cascade to multiple small-scale reconnection events. *Astron. Astrophys.* **525**, A57.

Redner, S. 2001 *A guide to first-passage processes*. Cambridge, U.K.: Cambridge University Press.

Rudnick, J. & Hu, Y. 1987 The winding angle distribution for an ordinary random walk. *J. Phys. A* **20**, 4421–4438.

Spitzer, F. 1958 Some theorems concerning 2-dimensional Brownian motion. *Trans. Amer. Math. Soc.* **87**, 187–197.

Sumners, D. W. 2009 Random knotting: Theorems, simulations and applications. In *Lectures on Topological Fluid Mechanics* (ed. R. L. Ricca), pp. 187–217. Berlin: Springer.

Thiffeault, J.-L. 2005 Measuring topological chaos. *Phys. Rev. Lett.* **94** (8), 084502.

Thiffeault, J.-L. 2010 Braids of entangled particle trajectories. *Chaos* **20**, 017516.

Török, T., Berger, M. A. & Kliem, B. 2010 The writhe of helical structures in the solar corona. *Astron. Astrophys.* **516**, A49.

Tumasz, S. E. 2012 Topological stirring. PhD thesis, University of Wisconsin – Madison, Madison, WI.

Wilmot-Smith, A. L. & De Moortel, I. 2007 Magnetic reconnection in flux-tubes undergoing spinning footpoint motions. *Astron. Astrophys.* **473**, 615–623.

Wilmot-Smith, A. L., Pontin, D. I. & Hornig, G. 2010 Dynamics of braided coronal loops. I. Oonset of magnetic reconnection. *Astron. Astrophys.* **516**, A5.

Wilmot-Smith, A. L., Pontin, D. I., Yeates, A. R. & Hornig, G. 2011 Heating of braided coronal loops. *Astron. Astrophys.* **536**, A67.

Yeates, A. R. & Hornig, G. 2011 Dynamical constraints from field line topology in magnetic flux tubes. *J. Phys. A* **44**, 265501.